Search for Antihelium with the BESS-Polar Spectrometer

K. Abe *et al.*

Phys. Rev. Lett. **108**, 131301 — Published 29 March 2012

DOI: 10.1103/PhysRevLett.108.131301

Search for Antihelium with the BESS-Polar Spectrometer

K. Abe,[1] H. Fuke,[2] S. Haino,[3] T. Hams,[4] M. Hasegawa,[3] A. Horikoshi,[3] A. Itazaki,[1] K. C. Kim,[5] T. Kumazawa,[3] A. Kusumoto,[1] M. H. Lee,[5] Y. Makida,[3] S. Matsuda,[3] Y. Matsukawa,[1] K. Matsumoto,[3] J. W. Mitchell,[4] Z. Myers,[5] J. Nishimura,[6] M. Nozaki,[3] R. Orito,[1] J. F. Ormes,[7] K. Sakai,[6] M. Sasaki,[4,*] E. S. Seo,[5] Y. Shikaze,[1] R. Shinoda,[6] R. E. Streitmatter,[4] J. Suzuki,[3] Y. Takasugi,[1] K. Takeuchi,[1] K. Tanaka,[3] N. Thakur,[7] T. Yamagami,[2] A. Yamamoto,[3,6] T. Yoshida,[2] and K. Yoshimura[3]

[1] *Kobe University, Kobe, Hyogo 657-8501, Japan.*
[2] *Institute of Space and Astronautical Science, Japan Aerospace Exploration Agency (ISAS/JAXA), Sagamihara, Kanagawa 252-5210, Japan.*
[3] *High Energy Accelerator Research Organization (KEK), Tsukuba, Ibaraki 305-0801, Japan.*
[4] *NASA/Goddard Space Flight Center, Greenbelt, MD 20771, USA.*
[5] *University of Maryland, College Park, MD 20742, USA.*
[6] *The University of Tokyo, Bunkyo, Tokyo 113-0033 Japan.*
[7] *University of Denver, Denver, CO 80208, USA.*

(Dated: February 29, 2012)

In two long-duration balloon flights over Antarctica, the BESS-Polar collaboration has searched for antihelium in the cosmic radiation with the highest sensitivity reported. BESS-Polar I flew in 2004, observing for 8.5 days. BESS-Polar II flew in 2007-2008, observing for 24.5 days. No antihelium candidate was found in BESS-Polar I data among 8.4×10^6 $|Z| = 2$ nuclei from 1.0 to 20 GV or in BESS-Polar II data among 4.0×10^7 $|Z| = 2$ nuclei from 1.0 to 14 GV. Assuming antihelium to have the same spectral shape as helium, a 95% confidence upper limit to the possible abundance of antihelium relative to helium of 6.9×10^{-8} was determined combining all BESS data, including the two BESS-Polar flights. With no assumed antihelium spectrum and a weighted average of the lowest antihelium efficiencies for each flight, an upper limit of 1.0×10^{-7} from 1.6 to 14 GV was determined for the combined BESS-Polar data. Under both antihelium spectral assumptions, these are the lowest limits obtained to date.

The existence of antiparticles was predicted by Dirac [1] and confirmed by Anderson through discovery of the positron in the cosmic radiation [2]. Antiprotons were later produced in high-energy proton interactions at accelerators [3]. The same process was expected to produce cosmic ray antiprotons from interactions of primary nuclei with the interstellar gas, but the first reported detections [4, 5] were not definitive. More advanced magnetic-rigidity spectrometers unambiguously identified antiprotons in the cosmic radiation [6–8] and they have now become important tools for investigating other phenomena [9–11]. The production of antinuclei with $|Z| = 2$ in collisions of high-energy nuclear beams has now been confirmed [12]. However, there is no evidence of antinuclei with $|Z| \geq 2$ in the cosmic radiation [13] or, by implication, in the cosmological neighborhood.

The apparent asymmetry of particles and antiparticles is one of the fundamental problems in cosmology. This was probably caused by symmetry-breaking between particles and antiparticles just after the Big Bang, with cosmological antiparticles vanishing at an early stage of the universe. Local symmetry breaking is not excluded and antimatter domains could remain. However, searches for annihilation signatures in the diffuse gamma-ray background and CMB distortions have shown that there are no large antimatter regions in the visible universe [14]. Relatively small pockets of primordial antimatter are not excluded [15, 16] and antinuclei might reach Earth from such regions. The BESS collaboration has searched for antinuclei in the cosmic radiation since 1993, with eight conventional one-day balloon flights and two long-duration Antarctic flights.

The BESS-Polar magnetic-rigidity spectrometer was developed for precise measurements of cosmic-ray antiprotons to low energies and to search for antihelium ($\overline{\mathrm{He}}$) with great sensitivity [9–11]. Versions made long-duration balloon flights over Antarctica in 2004 (BESS-Polar I) and 2007-2008 (BESS-Polar II). BESS-Polar is configured to extend measurements down to 100 MeV [10]. To reduce material encountered by incident particles, no pressure vessel is used and the magnet wall thickness is half that of BESS [17]. The time-of-flight (TOF) detectors and aerogel Cherenkov counter (ACC), with their front-end electronics, operate in vacuum. The magnet cryostat is the pressure vessel for the central tracker [18]. For BESS-Polar II, a new magnet with greater liquid helium capacity and improved thermal performance enabled extended observations.

Figure 1 shows schematic cross-sectional and side views of the BESS-Polar II spectrometer. All the detector components are arranged in a cylindrical configuration to maximize geometric acceptance. The TOF scintillators, 10 upper (UTOF) and 12 lower (LTOF), measure incident particle velocities β with a time resolution of 120 ps, and give independent $\mathrm{d}E/\mathrm{d}x$ measurements. Photomultiplier tubes (PMTs) are coupled to both ends of the scintillators. An additional TOF layer (MTOF) is installed between the bottom Inner Drift Chamber (IDC)

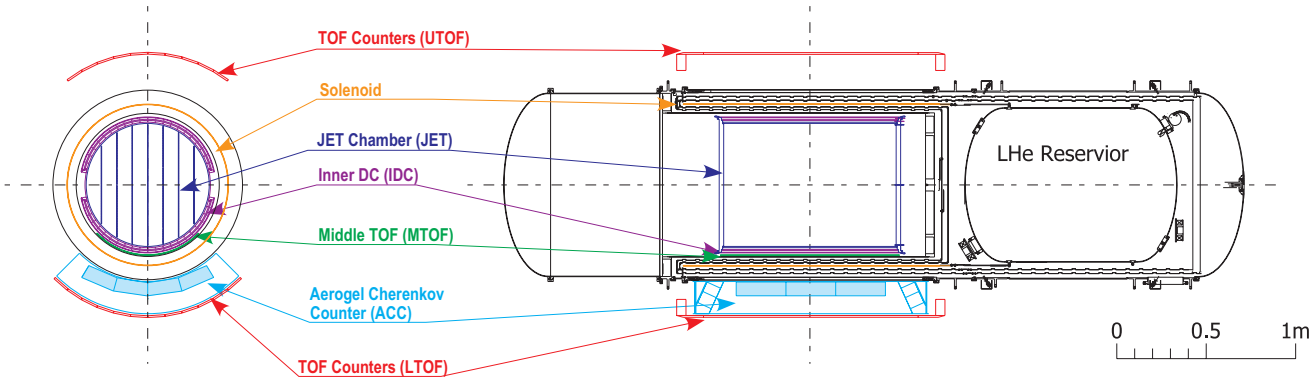

FIG. 1. Cross-sectional and side views of the BESS-Polar II Spectrometer.

and warm bore to detect low energy particles that cannot penetrate the lower magnet wall. Events are triggered by the UTOF in coincidence with LTOF or MTOF and recorded without in-flight selection. The ACC is located between the magnet and the LTOF to separate antiproton events from e^- and μ^- background. The MTOF and ACC are not used for the $\overline{\text{He}}$ search.

The superconducting solenoid provided a uniform field of 0.8 Tesla for over 11 days of continuous operation in BESS-Polar I and over 25 days in BESS-Polar II. Two IDCs and a JET-cell type drift chamber (JET) using continuously refreshed CO_2 are located inside the warm bore (0.80 m in diameter and 1.4 m in length). The axial positions of incident particles are initially determined using the UTOF and LTOF then refined using the JET and IDC. In the bending plane, particle trajectories are fit using up to 52 points, each with 140 μm resolution. The resulting magnetic-rigidity (R $\equiv$ p/Z, momentum divided by electric charge) resolution is 0.4% at 1 GV, with a maximum detectable rigidity (MDR) of 240 GV. The JET also measures dE/dx.

BESS-Polar I was launched on 13 December 2004 from Williams Field near McMurdo Station, flying for 8.5 days and recording 900 million cosmic-ray events. Several PMTs on the TOF with high count rates and excessive current draw were turned off, but 66% of the full geometric acceptance was retained by modifying the trigger algorithm. BESS-Polar II was launched on 22 December 2007. It flew for 29.5 days and observed for 24.5 days at float altitude with the magnet energized, recording 4.7 billion events. Full geometric acceptance was maintained during the entire flight, although two TOF PMTs were turned off due to an HV control issue. After one day, full JET chamber HV could not applied and the gas pressure was adjusted to compensate. The position resolution of the JET chamber was maintained, using HV-dependent calibration over short time intervals, and overall tracking performance was comparable to BESS-Polar I.

To eliminate events in which more than one particle passed through the spectrometer and particles interacting in the instrument, events with a single good track were chosen. Only one track was allowed in the drift chamber, and one hit each in the UTOF and LTOF. Next, track quality selections were applied, including hit data consistency between TOF and drift chambers, trajectory fits with $\chi^2 \leq 2.5$ and detected track ≥ 500 mm, sufficient number of wire hits along the track, and fiducial cuts. More severe selections were applied for events lacking a full complement of IDC hits. The tracking cuts do not depend on particle charge-sign or rigidity.

He ($\overline{\text{He}}$) nuclei were identified by their absolute charge, $|Z|$ (from dE/dx), and mass, M, determined by:

$$M^2 = R^2 Z^2 (\frac{1}{\beta^2} - 1). \quad (1)$$

$1/\beta$ and dE/dx band cuts were used to select He ($\overline{\text{He}}$), as illustrated for the TOF in Figure 2. A similar cut was applied to dE/dx measured by the drift chamber.

Figure 3 shows the R^{-1} distribution of the BESS-Polar II $|Z| = 2$ data with all selections applied. The rigidity range for the $\overline{\text{He}}$ search is bounded by rapidly decreasing efficiency at the low end and at the high end by the finite rigidity resolution of the spectrometer. The highest negative rigidity was chosen to exclude the observed misidentification (spillover) of high-rigidity He. More He events increase the extent of the tail and restrict the search range. No $\overline{\text{He}}$ candidates were found in the rigidity range 1.0 to 20 GV, among 8.4×10^6 $|Z| = 2$ nuclei identified by BESS-Polar I, or in the rigidity range 1.0 to 14 GV, among 4.0×10^7 $|Z| = 2$ nuclei identified by BESS-Polar II. Only upper limits to the abundance ratio of $\overline{\text{He}}$/He at the top of the atmosphere (TOA) can be determined.

If $\overline{\text{He}}$ had been observed, the ratio corrected to TOA would have been:

$$R_{\overline{\text{He}}/\text{He}} = \frac{\int N_{Obs,\overline{\text{He}}}/(S\Omega \times \overline{\eta} \times \overline{\epsilon}_{sngl} \times \overline{\epsilon}_{dE/dx} \times \overline{\epsilon}_{\beta} \times \overline{\epsilon}_{DQ})\ dE}{\int N_{Obs,\text{He}}/(S\Omega \times \eta \times \epsilon_{sngl} \times \epsilon_{dE/dx} \times \epsilon_{\beta} \times \epsilon_{DQ})\ dE},$$

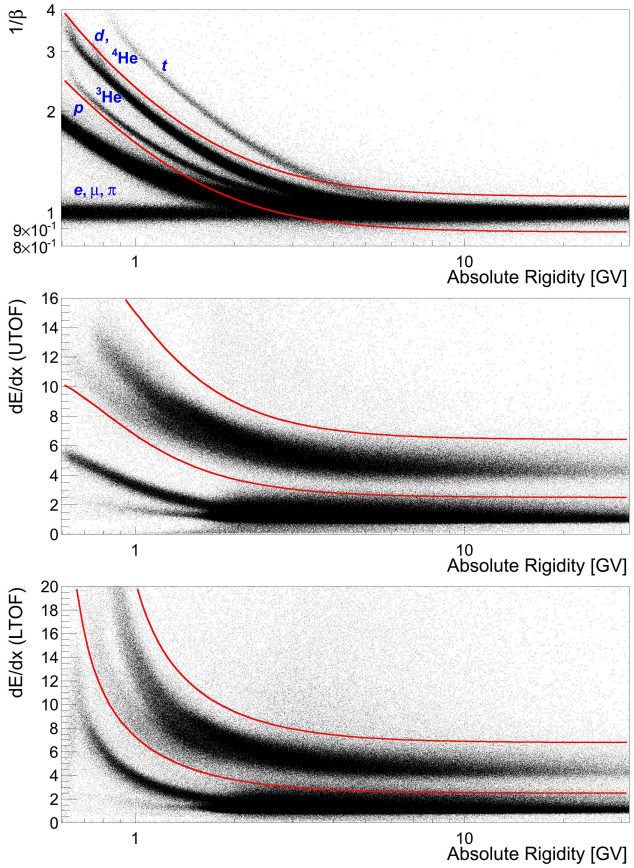

FIG. 2. Selection of He ($\overline{\text{He}}$) in BESS-Polar II. The upper panel shows β^{-1} vs absolute rigidity. The lower two panels show $\mathrm{d}E/\mathrm{d}x$ from the TOF vs absolute rigidity. The $|Z| = 2$ particles are between the lines.

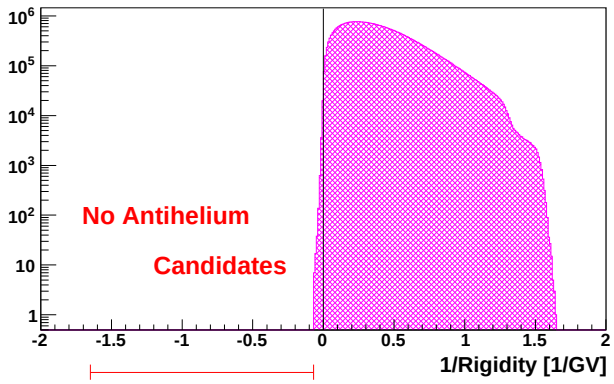

FIG. 3. R^{-1} distribution of $|Z| = 2$ events for BESS-Polar II. The negative 1/R events are spillover of He due to the finite spectrometer resolution. The "bump" around 1/R $\sim$ 1.4 is due to differing range-energy relationships of ^{4}He and ^{3}He.

(2)

where $N_{Obs,\mathrm{He}(\overline{\mathrm{He}})}$ is the differential intensity of observed He ($\overline{\text{He}}$) events, SΩ is geometric acceptance, η ($\overline{\eta}$) is the survival probability of He ($\overline{\text{He}}$) traversing the atmosphere, ϵ_{sngl} ($\overline{\epsilon}_{sngl}$) is the single track efficiency for He ($\overline{\text{He}}$), $\epsilon_{dE/dx}$ ($\overline{\epsilon}_{dE/dx}$) is the $\mathrm{d}E/\mathrm{d}x$ selection efficiency for He ($\overline{\text{He}}$), ϵ_β ($\overline{\epsilon}_\beta$) is the β selection efficiency for He ($\overline{\text{He}}$), and ϵ_{DQ} ($\overline{\epsilon}_{DQ}$) is the data quality selection efficiency for He ($\overline{\text{He}}$).

In order to calculate an upper limit, the energy dependent efficiencies for $\overline{\text{He}}$ must be determined. We consider two different assumptions for a hypothetical $\overline{\text{He}}$ energy spectrum.

1) Same spectral shape for $\overline{He}$ as for He:
If the shape of the hypothetical energy spectrum of $\overline{\text{He}}$ is assumed to be the same as for He, 3.1 (the maximum number of hypothetical $\overline{\text{He}}$ nuclei consistent at 95 % confidence with a null detection and no background [19]) is substituted for $\int N_{Obs,\overline{\mathrm{He}}}\, dE$, and factors are canceled that do not depend on charge-sign ($\epsilon_{dE/dx} = \overline{\epsilon}_{dE/dx}$, $\epsilon_\beta = \overline{\epsilon}_\beta$, and $\epsilon_{DQ} = \overline{\epsilon}_{DQ}$) then Equation 2 simplifies to:

$$R_{\overline{\mathrm{He}}/\mathrm{He}} < \frac{3.1}{\int N_{Obs,\mathrm{He}} \times \overline{\eta} \times \overline{\epsilon}_{sngl}/(\eta \times \epsilon_{sngl})\; dE}. \quad (3)$$

η ($\overline{\eta}$) and ϵ_{sngl} ($\overline{\epsilon}_{sngl}$) are determined using a Monte Carlo simulation with GEANT3/GHEISHA. The BESS-Polar I data give an upper limit for $R_{\overline{\mathrm{He}}/\mathrm{He}}$ of 4.4×10^{-7} from 1.0 to 20 GV, and the BESS-Polar II data give 9.4×10^{-8} from 1.0 to 14 GV. Combining the null detections in all BESS flights by summing their Equation 3 denominators gives an upper limit of 6.9×10^{-8} from 1.0 to 14 GV. The new limits are shown in Figure 4 together with previous results.

2) No assumed $\overline{He}$ spectrum:
The most conservative upper limit is obtained if no shape is assumed for the $\overline{\text{He}}$ spectrum and the lowest overall $\overline{\text{He}}$ efficiency within the search range is applied to any hypothetical $\overline{\text{He}}$. Because SΩ is nearly constant over the search range, Equation 2 then simplifies to:

$$R_{\overline{\mathrm{He}}/\mathrm{He}} < \frac{3.1 \;/\; [\overline{\eta} \times \overline{\epsilon}_{sngl} \times \overline{\epsilon}_{dE/dx} \times \overline{\epsilon}_\beta \times \overline{\epsilon}_{DQ}]_{MIN}}{\int N_{Obs,\mathrm{He}}/(\eta \times \epsilon_{sngl} \times \epsilon_{dE/dx} \times \epsilon_\beta \times \epsilon_{DQ})\; dE}, \quad (4)$$

The calculated overall $\overline{\text{He}}$ efficiencies are flat for most of the rigidities searched above, but decrease at lower rigidities due to annihilation. The ranges used here were adjusted to simultaneously optimize efficiencies and statistics. The resulting $\overline{\text{He}}$ spectrum independent upper limits are 5.3×10^{-7} from 1.5 to 20 GV for BESS-Polar I and 1.2×10^{-7} from 1.6 to 14 GV for BESS-Polar II, only about 25% higher than the corresponding limits calculated above. Data from the BESS-Polar flights were combined by summing the number of He and using a weighted average of the $\overline{\text{He}}$ efficiencies, giving a spectrum independent upper limit of 1.0×10^{-7} from 1.6 to

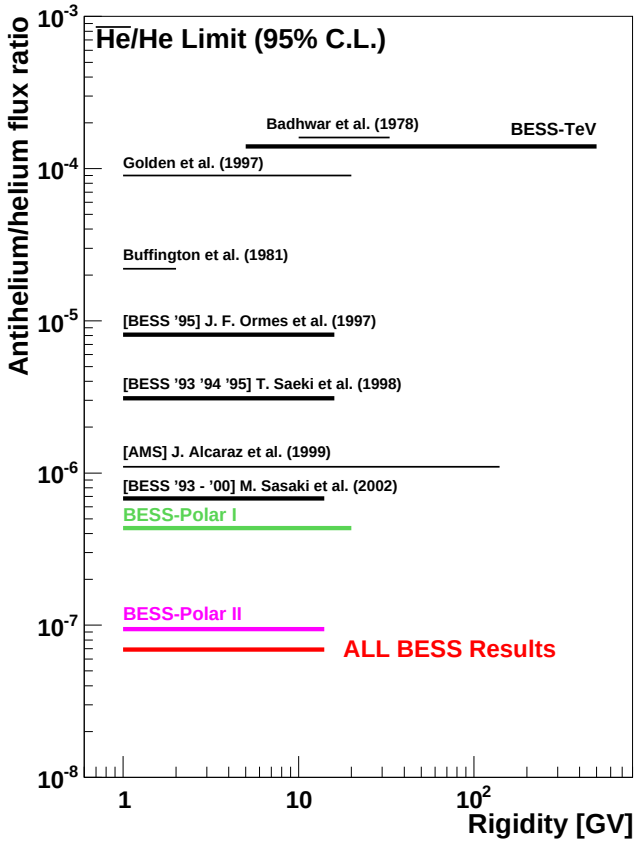

FIG. 4. The new upper limits of $\overline{He}$/He at the TOA calculated assuming the same energy spectrum for $\overline{He}$ as for He with previous experimental results ([13],[20],[21],[22],[23],[24],[25],[26]). The limit calculated with no spectral assumption is about 25 % higher.

14 GV. For the present work, earlier BESS flights were not reanalyzed under this assumption.

The BESS-Polar collaboration has established the lowest limits to date on the possible presence of $\overline{He}$ in the cosmic radiation.

The authors thank NASA Headquarters, ISAS/JAXA, and KEK for continuous support and encouragement in this United States-Japan project. We thank the NASA Balloon Program Office at GSFC/WFF, the NASA Columbia Scientific Balloon Facility, the National Science Foundation, and Raytheon Polar Services for their professional support of the Antarctic flights. BESS-Polar is supported in Japan by MEXT grants KAKENHI (13001004; 18104006), and in the U.S. by NASA (10-APRA10-0160; NNX10AC48G).

* Corresponding author. Email: Makoto.Sasaki@nasa.gov

[1] P. A. M. Dirac, Royal Society of London Proceedings Series A **117**, 610 (1928).

[2] C. D. Anderson, Phys. Rev. **43**, 491 (1933).

[3] O. Chamberlain, E. Segrè, C. Wiegand, and T. Ypsilantis, Phys. Rev. **100**, 947 (1955).

[4] R. L. Golden *et al.*, Phys. Rev. Lett. **43**, 1196 (1979).

[5] E. A. Bogomolov, N. D. Lubyanaya, V. A. Romanov, S. V. Stepanov, and M. S. Shulakova, in *Proceedings of the 16th International Cosmic Ray Conference, Kyoto, Japan*, Vol. 1 (1979) pp. 330–335.

[6] K. Yoshimura, S. Orito, I. Ueda, *et al.*, Physical Review Letters **75**, 3792 (1995).

[7] J. W. Mitchell, L. M. Barbier, E. Christian, *et al.*, Physical Review Letters **76**, 3057 (1996).

[8] M. Boezio, P. Carlson, T. Francke, N. Weber, *et al.*, Astrophys. J. **487**, 415 (1997).

[9] K. Abe *et al.*, Physical Review Letters **108**, 051102 (2012).

[10] J. W. Mitchell, A. Yamamoto, *et al.*, *Proceedings of the 31st International Cosmic Ray Conference, Łódź, Poland*, **Invited, Rapporteur and Highlight Papers**, 149 (2009).

[11] A. Yamamoto, J. W. Mitchell, K. Yoshimura, *et al.*, Adv. Space Res. (2011), 10.1016/j.asr.2011.07.012, in press.

[12] H. Agakishiev *et al.*, Nature (London) **473**, 353 (2011).

[13] M. Sasaki, S. Haino, *et al.*, Adv. Space Res. **42**, 450 (2008).

[14] A. G. Cohen, A. de Rujula, and S. L. Glashow, Astrophys. J. **495**, 539 (1998).

[15] M. Y. Khlopov, S. G. Rubin, and A. S. Sakharov, Phys. Rev. D **62**, 083505 (2000).

[16] A. D. Dolgov, Nucl. Phys. B (Proc. Suppl.) **113**, 40 (2002).

[17] Y. Ajima *et al.*, Nuclear Instruments and Methods in Physics Research A **443**, 71 (2000).

[18] S. Haino, T. Sanuki, *et al.*, Phys. Lett. B **594**, 35 (2004).

[19] G. J. Feldman and R. D. Cousins, Phys. Rev. D **57**, 3873 (1998).

[20] G. D. Badhwar, R. L. Golden, J. L. Lacy, J. E. Zipse, R. R. Daniel, and S. A. Stephens, Nature (London) **274**, 137 (1978).

[21] R. L. Golden, S. J. Stochaj, S. A. Stephens, A. A. Moiseev, J. F. Ormes, R. E. Streitmatter, T. Bowen, A. Moats, and J. Lloyd-Evans, Astrophys. J. **479**, 992 (1997).

[22] A. Buffington, S. M. Schindler, and C. R. Pennypacker, Astrophys. J. **248**, 1179 (1981).

[23] J. F. Ormes, A. A. Moiseev, T. Saeki, K. Anraku, S. Orito, *et al.*, Astrophys. J. **482**, L187+ (1997).

[24] T. Saeki, K. Anraku, S. Orito, J. Ormes, *et al.*, Phys. Lett. B **422**, 319 (1998).

[25] J. Alcaraz *et al.*, Phys. Lett. B **461**, 387 (1999).

[26] M. Sasaki *et al.*, Nucl. Phys. B (Proc. Suppl.) **113**, 202 (2002).